Molecular aggregations and supramolecular architectures of amphiphilic PEO_{17}–OPV_3 and its hybrid with silica

Chi-Chun Hsieh and King-Fu Lin*

Received 7th March 2005, Accepted 13th July 2005
First published as an Advance Article on the web 9th August 2005
DOI: 10.1039/b503393d

The synthesis, luminescence properties and self-assembly of a specifically-designed amphiphilic PEO_{17}–OPV_3 molecule (and its hybrid with silicates) to form ring-like disks are described. The synthesis was begun with the Wittig–Horner reaction to form a co-planar π-conjugated PPV oligomer segment, followed by linking with PEO_{17} through a sulfonate group that causes a twist in the molecule between the hydrophobic and hydrophilic segments. Due to its amphiphilic nature, its photoluminescence behavior is greatly affected by the solvent type and concentration. The deposition of PEO_{17}–OPV_3 molecules on mica with a proper co-solvent was able to form a ring-like supramolecular architecture of *ca.* 30 nm in diameter as observed by atomic force microscopy (AFM). The width of the enclosed peripheral area on both sides of the ring is on the same order of magnitude as the length of the PEO_{17}–OPV_3 molecule. The self-assembly of a PEO_{17}–OPV_3 hybrid with silica to form a ring-like disk of *ca.* 150 nm diameter and *ca.* 0.65 nm thickness was also observed. The latter is roughly equal to the width of rod segment, implying that π–π stacking governs the self-assembly process in the co-organization between PEO_{17}–OPV_3 molecules and silicates, whereas the twist in molecules orients the ring formation. As a result, a multi-lamellar phase transformation mechanism is proposed for the formation of such a supramolecular architecture.

Introduction

Among the series of π-conjugated polymers, polyphenylene–vinylene (PPV)-based polymers have been widely studied ever since their optoelectronic properties were discovered.[1,2] Recently, the ability of their oligomers (OPV) to form supramolecular architectures has attracted great attention because of potential application in optoelectronic nano-devices.[3–8] It is commonly accepted that the optoelectronic properties of π-conjugated molecules are affected not only by the primary molecular structure (π-conjugation) but by the supramolecular organization (π-stacking), similar to that of the proteins and block copolymers.[9–15] For example, Stupp *et al.*[16] have found that the self-assembly of the conjugated molecules into supramolecular ribbon nanostructures leads to enhanced electronic conductivity due to improved π-orbital overlap. In this aspect, amphiphilic molecules with a proper hydrophilicity or hydrophobicity are needed to proceed with a self-assembly process. Researches in the field of self-assembly techniques usually focus first on the design and synthesis of self-assembling amphiphilic or liquid-crystalline molecules, followed by the investigation of aggregation behavior in the liquid as well as the solid state.[17–33]

In this work, we have synthesized a specifically designed amphiphilic PEO_{17}–OPV_3 molecule with a rigid OPV segment linking with a soft PEO segment through a sulfonate group that twists the molecule between hydrophilic and hydrophobic segments. PEO_{17}–OPV_3 is also a blue-light emitting molecule, owing to the existence of a conjugated OPV_3 segment. Its aggregation in both polar and apolar solvents has a great influence on its light-emitting properties, as revealed by the fluorescence spectroscopy. By deposition on mica under proper preparation conditions, a ring-like supramolecular structure of *ca.* 30 nm in diameter was observed by atomic force microscopy (AFM). Although the ring structures have always been observed in di- or tri- block copolymer assemblies,[34,35] they were rarely reported for the amphiphilic conjugated oligomer systems. Instead, cylindrical, tubular, and fibril supramolecular structures were consistently reported.[3–8,36]

On the other hand, since the discovery of the M41 family of silicate mesoporous molecular sieves by Mobil researchers in 1992,[37] surfactant-templated silica or titania with ordered nanostructures become a promising candidate for optoelectronic devices such as solar cells.[38] Considering that the amphiphilic PEO_{17}–OPV_3 molecule itself is also a surfactant, it might be used as a template to construct the hybrid nanostructures with nanopatterns served for the nano-sized devices. To this end, we prepared a solution of pre-gelled (PEO_{17}–OPV_3)–silica hybrid materials and allowed them to deposit on mica. A thin ring-like disk of *ca.* 150 nm in diameter and *ca.* 0.65 nm in thickness was observed by AFM. The thickness is roughly equal to the width of the hydrophobic rod segment of the PEO_{17}–OPV_3 molecule. Since the supramolecular structure of the hybrid is similar to that of the neat amphiphilic molecule, PEO_{17}–OPV_3 is considered to play a structure-directing role for the hybrid materials.

Department of Materials Science and Engineering, National Taiwan University, Taipei, Taiwan, Republic of China.
E-mail: kflin@ccms.ntu.edu.tw; Fax: +886 2 2363 4562;
Tel: +886 2 2392 8290

Experimental

Materials

All starting materials were purchased from commercial suppliers (Acros and Aldrich). Tetrahydrofuran (THF) was dried and distilled over sodium. All used solvents were degassed by sparkling with nitrogen for 30 min prior to use.

Dibutyl(4-*tert*-butylphenyl)methylphosphonate (1). In a flask with a magnetic stirring bar was placed 2 mL (10 mmol) 1-*tert*-butyl-4-(chloromethyl)benzene and 8 g (30 mmol) tributyl phosphate. The reaction mixture was stirred and refluxed at 160 °C under nitrogen for 12 h. After cooling to room temperature, the mixture was concentrated under reduced pressure at 200 °C to remove the residual tributyl phosphate. The resulting yellow oil was used for the next Horner–Wittig reaction without further purification. Yield: 80%. ^{1}H NMR (500 MHz, $CDCl_3$): δ(ppm): 7.08–7.32 (m, 4H), 3.99 (t, 4H), 3.77 (m, 2H), 1.57 (m, 4H), 1.45 (m, 4H), 1.34 (s, 9H), 0.91 (t, 6H).

4-(4-*tert*-butylstyryl)benzaldehyde (2). A solution of 3.44 g (16 mmol) 4-(diethoxymethyl)benzaldehyde and 4.8 g (14 mmol) phosphonate (**1**) in 30 mL THF was prepared in a flask with a magnetic stirring bar and added dropwise with potassium *t*-butoxide solution in THF (1.8 g, 60 mL). The mixture was stirred for 18 h at room temperature under nitrogen. Then, 50 mL of 37.5% HCl was added and the mixture was stirred for another 3 h. Afterwards, the reaction mixture was poured into a 500 mL water–ethanol (1 : 1 by volume) for precipitation. The precipitates were filtered and washed with water and ethanol for several times. Recrystallization from dichloromethane–ethanol gave a pure yellow solid product. Yield: 70%. ^{1}H NMR (500 MHz, $CDCl_3$): δ(ppm): 9.97 (s, 1H), 7.84 (d, 2H), 7.62 (d, 2H), 7.47 (d, 2H), 7.40 (d, 2H), 7.23 (d, 1H), 7.10 (d, 1H), 1.33 (s, 9H).

Dibutyl(4-sulfonyl chloride phenyl)methylphosphonate (3). In a flask with a magnetic stirring bar was placed 1 g (3.7 mmol) of 4-(bromomethyl)benzene-1-sulfonyl chloride and 3 g (12 mmol) of tributyl phosphate. The reaction mixture was stirred and refluxed at 160 °C under nitrogen for 12 h. After cooling to room temperature, the mixture was concentrated under reduced pressure at 200 °C to remove the residual tributyl phosphate. The resulting brown oil was used for the next Horner–Wittig reaction without further purification. Yield: 90%. ^{1}H NMR (500 MHz, $CDCl_3$): δ(ppm): 7.03–7.40 (m, 4H), 4.00 (m, 4H), 3.03 (m, 2H), 1.61 (m, 4H), 1.59 (m, 4H), 0.89 (t, 6H).

OPV trimer end-capped with *tert*-butyl and sulfonyl chloride groups (4). A solution of 0.25 g (1.9 mmol) aldehyde (**2**) and 0.5 g (2.5 mmol) phosphonate (**3**) in 30 mL THF was prepared in a flask with a magnetic stirring bar and added dropwise with potassium *t*-butoxide solution in THF (0.34 g, 50 mL). The mixture was stirred for 18 h at room temperature under nitrogen. Then, 20 mL of 37.5% HCl was added and the mixture was stirred for another 3 h. Afterwards, the reaction mixture was poured into a 500 mL water for precipitation. The precipitates were filtered and washed with water several times. Recrystallization from chloroform gave a dark brown solid product. Yield: 65%. ^{1}H NMR (500 MHz, $CDCl_3$): δ(ppm): 8.15 (d, 2H), 7.59 (d, 2H), 7.43 (d, 2H), 7.38 (d, 2H), 7.21 (m, 4H), 7.11 (d, 4H), 1.31 (s, 9H).

Synthesis of PEO_{17}–OPV_3 (5). A solution of 0.3 g (0.4 mmol) poly(ethylene glycol) methyl ether (M_w = 750 g mol^{-1}) and 0.22 g (0.5 mmol) OPV trimer (**4**) in 150 mL dry dichloromethane was prepared in a flask with a magnetic stirring bar under nitrogen atmosphere and added dropwise with pyridine (1 g in 20 mL dry dichloromethane). The mixture was stirred for 36 h at room temperature. Afterwards, the mixture was washed with 50 mL water three times and then dried over $MgSO_4$. After removing the solvent with a vacuum evaporator, dark viscous oil was obtained. For purification, the crude product was subjected to column chromatography using ethyl acetate as an eluent. A purified light yellow oil product was obtained with a yield of 25%. ^{1}H NMR (500 MHz, $CDCl_3$): δ(ppm): 7.05–8.05 (m, 16H), 3.61 (m, 68H), 3.33 (s, 3H), 1.33 (s, 9H).

Preparation of amphiphilic PEO_{17}–OPV_3 solution samples for measurements of fluorescence spectroscopy

Stock solutions (100 mL) of 1.08×10^{-2} M in toluene and water were prepared first by dissolving 1.25 g PEO_{17}–OPV_3 to the respective solvents. For toluene, the stock solution was further diluted to 9.46×10^{-3}, 8.6×10^{-3}, 6.75×10^{-3}, 5.56×10^{-3}, 4.3×10^{-3}, 3.38×10^{-3}, 2.15×10^{-3}, 1.08×10^{-3}, 9.46×10^{-4}, 8.6×10^{-4}, 6.75×10^{-4}, 5.56×10^{-4}, 4.3×10^{-4}, 3.38×10^{-4}, 2.15×10^{-4}, 1.08×10^{-4}, 9.46×10^{-5}, 8.6×10^{-5}, 6.75×10^{-5}, 5.56×10^{-5}, 4.3×10^{-5}, 3.38×10^{-5}, 2.15×10^{-5}, 1.08×10^{-5} (M). For water, the stock solution was diluted to 5.56×10^{-3}, 4.3×10^{-3}, 3.38×10^{-3}, 2.15×10^{-3}, 1.08×10^{-3}, 9.46×10^{-4}, 8.6×10^{-4}, 6.75×10^{-4}, 5.56×10^{-4}, 4.3×10^{-4}, 3.38×10^{-4}, 2.15×10^{-4}, 1.08×10^{-4}, 9.46×10^{-5}, 8.6×10^{-5}, 6.75×10^{-5}, 5.56×10^{-5}, 4.3×10^{-5}, 3.38×10^{-5}, 2.15×10^{-5}, 1.08×10^{-5} (M). An excitation wavelength of 340 nm was chosen for the photoluminescence measurements.

Preparation of amphiphilic PEO_{17}–OPV_3 samples for AFM observation

The solution was prepared by dissolving PEO_{17}–OPV_3 in water–THF (1 : 1 by volume) at a concentration of 3.38×10^{-5} M. An automatically-flat mica disk was placed into the prepared solution in a Petri dish and maintained in level position for 48 h. After the solution was removed with a dropper, the sample-deposited mica was then conditioned at ambient environment for 24 h, followed by thermal annealing at 120 °C in vacuum oven for 12 h.

Preparation of silicate source solution

In a vial, 2.7 mmol ethanol, 7.2 mmol water, and 0.12 mmol HCl were mixed with stirring at room temperature, and then added to 0.9 mmol tetraethyl orthosilicate (TEOS) in an ice bath by vigorously stirring to prevent gelation. The solution

was maintained in an ice bath under vigorous stir for 2 h to afford a silicate source solution.

Preparation of (PEO_{17}–OPV_3)–silicate hybrid samples for AFM observation

A solution of 0.2 g (0.17 mmol) PEO_{17}–OPV_3 in 5 mL THF was vigorously stirred for 30 min while the silicate source solution (0.9 mmol TEOS, 2.7 mmol ethanol, 7.2 mmol water, and 0.12 mmol HCl) was added dropwise. The mixture was heated to 60 °C with stirring and maintained for 90 min. Afterward, the mixture was diluted by 2 mL EtOH and 1 mL water before allowed to react for another 24 h at room temperature. The molar composition was 1.0 TEOS : 77 THF : 69 H_2O : 0.13 HCl : 0.19 PEO_{17}–OPV_3 : 51.9 EtOH. To prepare a thin film for AFM observation, 1 mL of the above solution was further diluted by 3 mL THF and 6 mL water in a Petri dish and an automatically-flat mica disk was placed into the solution and maintained in flat position for 48 h. Then, the solution was removed with a dropper. The sample-deposited mica was conditioned at ambient environment for 24 h, followed by thermal annealing at 120 °C in vacuum oven for 24 h.

Characterization

^{1}H Nuclear magnetic resonance (NMR) spectra were obtained in deuterated chloroform using a BRUKER DMX-500 MHz FT-NMR. Chemical shifts were referred to tetramethylsilane.

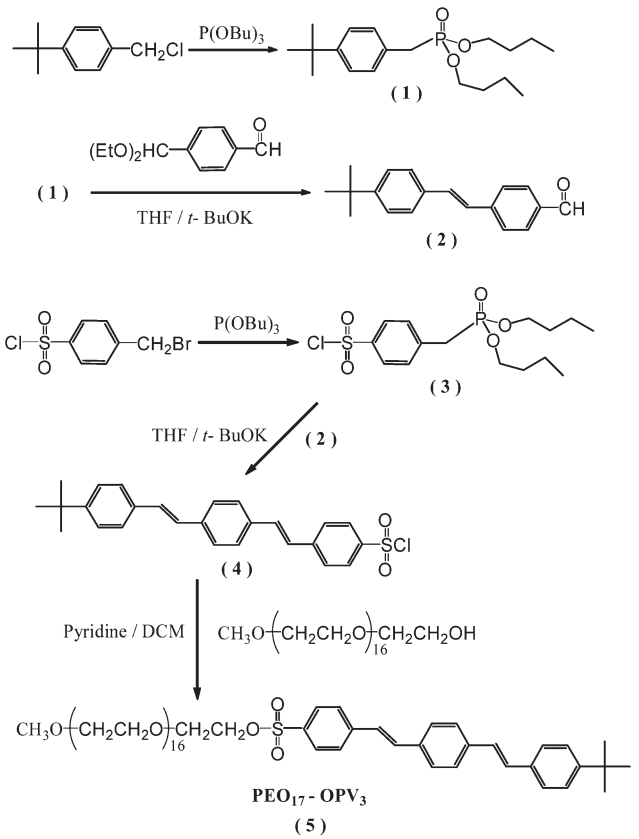

Fig. 1 Scheme for synthesis of the amphiphilic PEO_{17}–OPV_3 molecule.

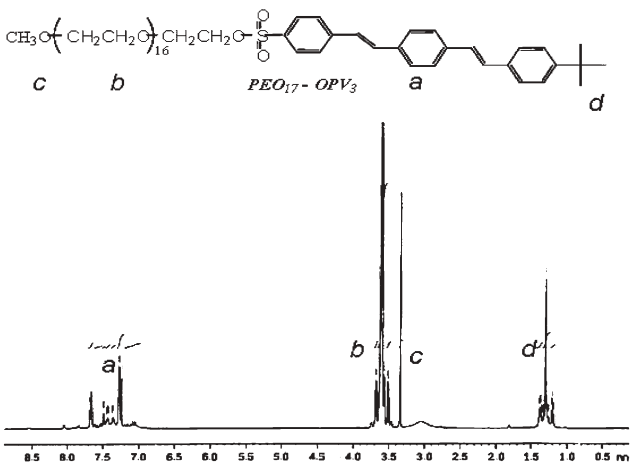

Fig. 2 ^{1}H NMR spectrum of the amphiphilic PEO_{17}–OPV_3 molecule.

Photoluminescence (PL) spectra were obtained by using a JASCO FP-777 spectrofluorometer at an excitation wavelength of 340 nm. The nanostructures on mica were investigated with AFM by using a Digital Instruments Dimension-3100 Multimode microscopes in tapping mode. The molecular model was constructed using a Cerius 2 energy minimization.

Results and discussion

Amphiphilic PEO_{17}–OPV_3 molecule

The scheme for the synthesis of the PEO_{17}–OPV_3 molecule is shown in Fig. 1, beginning with the Horner–Wittig reaction to form a co-planar π-conjugated *trans*-phenylene vinylene oligomer, followed by linking with PEO_{17} through a sulfonate group. Notably, the PPV trimer is recognized as a co-planar *trans*-linkage structure because no resonance at δ = 6.5–6.8 ppm in the ^{1}H NMR spectrum attributable to the *cis*-vinylene protons[39,40] was detected (Fig. 2). Besides, it is generally accepted that the conjugated vinylene bond formed using the Horner–Wittig reaction between an aromatic phosphonate ester and an aromatic aldehyde is normally in the *trans*-form.[36,41] Fig. 3 presents its 3-D primary structure, constructed by a Cerius 2 energy minimization. As seen in

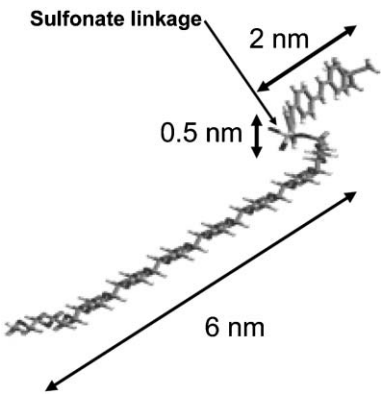

Fig. 3 Molecular graphics of the amphiphilic PEO_{17}–OPV_3 using a Cerius 2 energy minimization (arrow indicates sulfonate linkage).

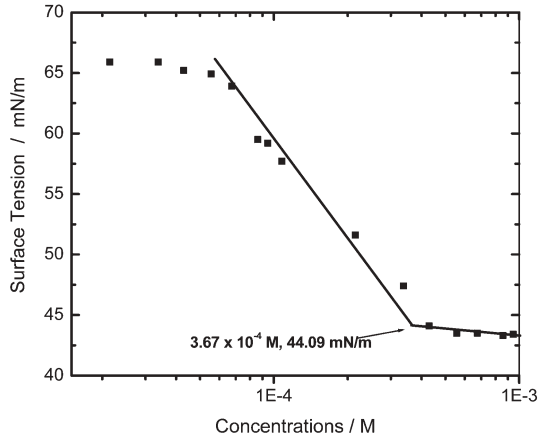

Fig. 4 Concentration dependence of surface tension for PEO_{17}–OPV_3 aqueous solutions.

the figure, the size of the OPV rod segment is about 2 nm in length and 0.5 nm in width, whereas the length of the extended PEO segment is about 6 nm. Interestingly, the as-tetrahedral shape of the sulfonate linking group caused a twist in the molecule between hydrophobic and hydrophilic segments. Due to the soft nature of the PEO segment, PEO_{17}–OPV_3 is also considered as a rod–coil molecule. Undoubtedly, both amphiphilic and rod–coil characters play major roles on the formation of self-assembling supramolecular structure.

Molecular aggregations and luminescence properties in the solution

A critical aggregation concentration (CAC) value of 3.67×10^{-4} M for PEO_{17}–OPV_3 in water was determined by surface tension meter (as shown in Fig. 4). It is believed that above the CAC, molecular aggregation to larger domains occurs. With a hydrophilic long segment linking the hydrophobic PPV conjugated segment, PEO_{17}–OPV_3 could dissolve in both polar and apolar solvents. In water (as shown in Fig. 5), excimer-like emission at 445 nm was dominant in dilute solution. With increasing concentration, the shoulder peak of

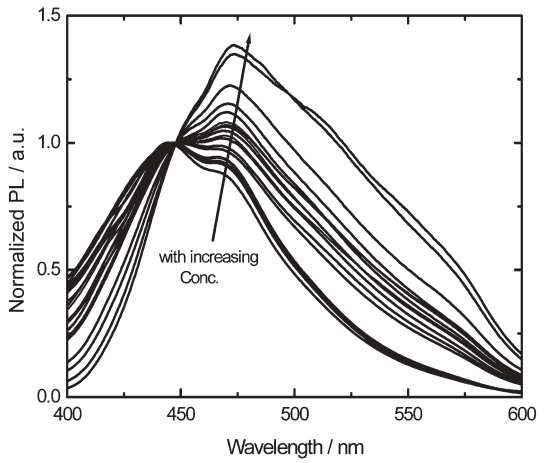

Fig. 5 Normalized PL spectra of PEO_{17}–OPV_3 in water at various concentrations, c (1.08×10^{-5} M $< c <$ 5.56×10^{-3} M), individually as replotted in Fig. 7.

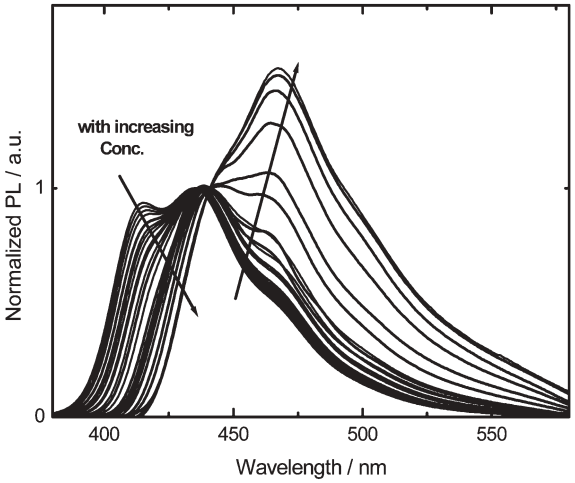

Fig. 6 Normalized PL of PEO_{17}–OPV_3 in toluene at various concentrations, c (1.08×10^{-5} M $< c <$ 1.08×10^{-2} M), individually as replotted in Fig. 7.

474 nm turned into the major peak as a result of forming large aggregates or supramolecular structures. On the other hand, in toluene (as shown in Fig. 6), typical 0–0 and 1–0 vibrational peaks located at 415 and 435 nm were observed in dilute solution. As concentration was increased, 0–0 vibrational peak that was often attributed to the molecularly dispersed emission, gradually disappeared due to the formation of excimers. Meanwhile, the second peak shifted to 440 nm and became the major peak in the concentration (c) range: 3.38×10^{-4} M $< c <$ 4.3×10^{-3} M. Finally, the major peak shifted to 471 nm as $c > 5.56 \times 10^{-3}$ M. At this point, it is reasonable to make a conjecture that a larger molecular-packing structure was formed and had a different photophysical emission center from the excimers. From the plot of relative intensities (as shown in Fig. 7, I_{474nm}/I_{445nm} for water and I_{471nm}/I_{440nm} for toluene), two-step slopes for the increase of relative intensities were found. Interestingly, the intersection for water was located at *ca.* 5×10^{-4} M near the CAC value determined by a surface tension meter. It indicates that the PL

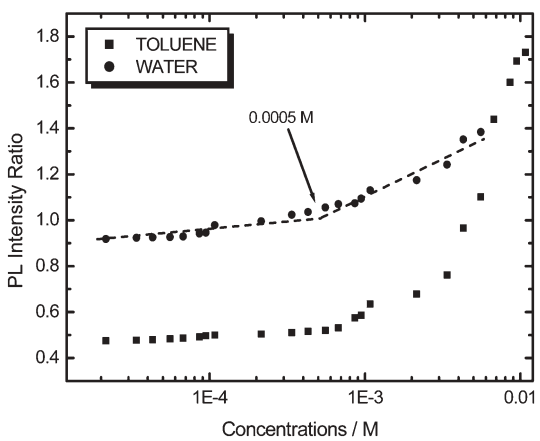

Fig. 7 Concentration dependences of PL intensity ratios for PEO_{17}–OPV_3 in water estimated by I_{474nm}/I_{445nm} and in toluene by I_{471nm}/I_{440nm}.

measurements are able to detect the formation of supramolecular structures.

Solid-state self-assembly from a PEO_{17}–OPV_3 solution

In this study, AFM was used to investigate the supramolecular architectures. Fig. 8 shows a ring-like structure with an average diameter of 30 nm deposited on mica from a solution of PEO_{17}–OPV_3 in water–THF (1 : 1 by volume) at a concentration of 3.38×10^{-5} M. Ring-like assemblies are not observed by accident but all over the mica substrate. The width of enclosed periphery area on both side of the ring ranging from 6 to 12 nm is the same order of magnitude as the length of PEO_{17}–OPV_3 molecule. Thus, we propose that this enclosed periphery area has a core–shell morphology with the OPV rigid segments forming the core and the PEO soft segments forming the shell. The top view of supramolecular model is schematically shown in Fig. 9 (top). The grey part represents the rigid OPV core and the black represents the soft PEO shell. To our knowledge, the formation of these self-assembled supramolecular structures might be influenced by the hydrophilicity of the mica surface.

Owing to the strong polarity of the mica surface, hydrophilic PEO segments have a tendency to lie flat on the surface, whereas the hydrophobic OPV segments tilts with its co-planar configuration normal to the surface. As mentioned in the Introduction section, most of the research groups studying the supramolecular structures of oligo-PPV observed structures with high aspect ratios, such as fibril or cylindrical textures,[28–33,36] significantly different from our observations. Two factors are possibly involved in the formation of ring structures: (1) the twist of molecules in between hydrophobic and hydrophilic segments forces them to have only one side with the same curvature to proceed with π–π stacking, and: (2) the high interfacial tension between mica and hydrophobic OPV segments causes the π–π stacking region to curl in order to reduce the interfacial area. Thus, thermodynamically, the packing region of hydrophobic OPV segments prefers to form a ring structure, unless the adhesion strength of hydrophilic PEO segments to mica is able to overcome this tendency. Besides, packing under the same curvature would favor the formation of a ring. After all, since thermal annealing of the deposited mica at 120 °C afforded a better image of the ring structures, these self-assembled supramolecular structures are thermodynamically stable.

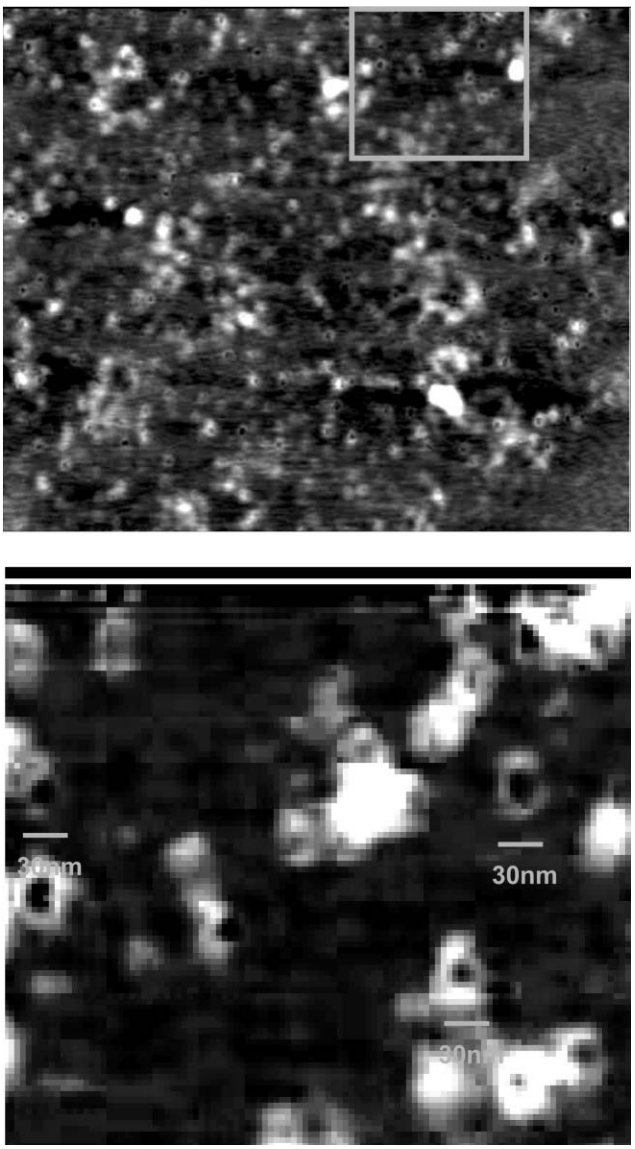

Fig. 8 AFM image of amphiphilic PEO_{17}–OPV_3 deposited on a mica substrate. Top: Image size is 2×2 μm. Bottom: enlarged image from the selection area of the top image.

Solid-state self-assembly from a (PEO_{17}–OPV_3)–silica hybrid solution

The hybrid solution was prepared by addition of a pre-gelled silicate source solution (0.9 mmol TEOS, 2.7 mmol ethanol, 7.2 mmol water, and 0.12 mmol HCl) to PEO_{17}–OPV_3 in THF.

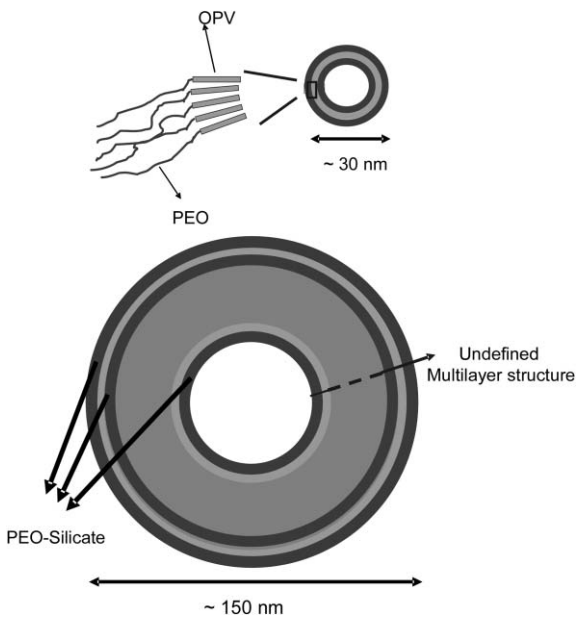

Fig. 9 Illustration of the supramolecular structure of neat amphiphilic PEO_{17}–OPV_3 molecule (top) and (PEO_{17}–OPV_3)–silicate hybrid (bottom).

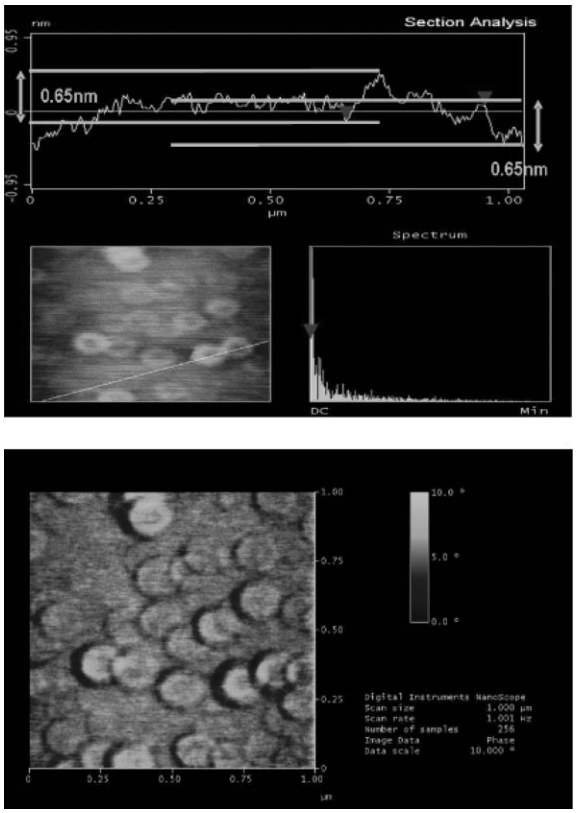

Fig. 10 AFM images of the (PEO_{17}–OPV_3)–silicate hybrid deposited on a mica substrate. Top: image analysis of 1 × 1 μm size. Bottom: phase image.

After reaction and dilution at proper conditions (see the Experimental section for a detailed description), a ring-like thin disk form of supramolecular architecture was deposited on mica as presented in Fig. 10. Although the supramolecular structure of the (PEO_{17}–OPV_3)–silica hybrid is approximately similar to that prepared from the neat PEO_{17}–OPV_3 solution, the diameter (*ca.* 150 nm) is much larger and more uniform. The thickness of *ca.* 0.65 nm measured from the image analysis of AFM (see Fig. 10 (top)) was also uniform. Notably, the thickness is roughly equal to the width of co-planar configuration of an OPV_3 rod segment (see Fig. 3), indicating that the π–π stacking of amphiphilic PEO_{17}–OPV_3 molecules acts as a template for the formation of the supramolecular structure of (PEO_{17}–OPV_3)–silica hybrid.

The exact mechanism of ring-like thin supramolecular architecture formation is not clear. However, we believe that at least three criteria listed below should be followed for this formation. First, PEO_{17}–OPV_3 molecules dissolving in solution in the first step of sample preparation should not have a tight packing for either the hydrophobic or hydrophilic segments. Otherwise, further organization to a larger supramolecular architecture becomes difficult. Thus, THF, a good solvent for both segments, was used. Second, the condensation reactions of TEOS through hydrolysis by HCl to form silicate oligomers should not go over 25% of total reacting groups. Otherwise, a three dimensional network forms and condenses as a small gelled particle.[42] A large scale gelation occurs as the extent of reactions reaches 33%.[42] Third, only the silicate oligomers that participate in the formation of supramolecular architectures are allowed to deposit on mica in the second step of sample preparation. The silicate oligomers that have no interaction with PEO_{17}–OPV_3 molecules remain in solution and should be removed as much as possible after deposition of supramolecular architectures.

Because a large amount of water is incorporated with the solution in the second step of sample preparation, OPV_3 segments pack tightly with each other. Some of the silicates are attracted to the neighborhood of PEO layers and interweave with the PEO segments to form a mutilamellar mesophase. It is highly possible that the ring-like thin supramolecular architectures were preformed in the solution before deposition on the mica surface, because they stacked with each other instead of fusing together (see Fig. 10 (bottom)). The width of the enclosed peripheral area on both sides of the rings is *ca.* 40 nm, several times larger than that formed by neat PEO_{17}–OPV_3 molecules (see Fig. 8). Since the thickness of ring-like supramolecular architectures is roughly equal to the width of co-planar configuration of an OPV_3 rod segment, π–π stacking of OPV_3 rod segments should govern the self-assembly process. The incorporation of silicate oligomers barely increased the thickness of ring over the width of OPV_3 rod segment. Furthermore, because silicate oligomers can perform crosslinking reactions, they act as a strong adhesive to bind several self-assembling PEO_{17}–OPV_3 supramolecular layers into a larger ring. The final supramolecular architecture of the (PEO_{17}–OPV_3)–silica hybrid is shown schematically in Fig. 9 (bottom).

A well self-assembled ring-like thin architecture of the (PEO_{17}–OPV_3)–silica hybrid with a diameter of *ca.* 150 nm and a thickness of *ca.* 0.65 nm will have many potential applications to nano-sized optoelectronic devices, such as nano-photodiodes, nano-switches, nano-computation devices, organic light emitting diodes, photovoltaic devices, *etc.*, if each ring can be manipulated individually. To realize these future applications, further researches in cooperation with physicists and electronic engineers are ongoing.

Conclusions

An amphiphilic rod–coil PEO_{17}–OPV_3 molecule was specifically designed with a sulfonate group linking between hydrophobic and hydrophilic segments that twists the molecule *in situ*. Its photoluminescent properties in solution were dependent on the solvent type and concentration in association with molecular aggregation. As it was deposited on mica surface, the π–π stacking of apolar co-planar OPV segments was forced to tilt normal to the mica surface, driving the self-assembly process to form a ring-like architecture with a diameter of *ca.* 30 nm. As it was blended with silicates in solution, a uniform ring-like thin disk of *ca.* 150 nm in diameter and *ca.* 0.65 nm in thickness was deposited on mica. Because the thickness is roughly equal to the width of co-planar OPV configurations, the silicates were believed to act as an adhesive that binds several self-assembled PEO_{17}–OPV_3 lamellae to form a larger ring-like supramolecular architectures. Its potential applications in nano-sized optoelectronic devices are under exploration.

Acknowledgements

The authors acknowledge the financial support of the National Science Council in Taiwan, Republic of China, through Grant NSC 92-2216-E-002-011.

References

1 J. H. Burroughes, D. D. C. Bradley, A. R. Brown, R. N. Marks, K. Mackay, R. H. Friend, P. L. Burns and A. B. Holmes, *Nature*, 1990, **347**, 539; D. Braun and A. J. Heeger, *Appl. Phys. Lett.*, 1991, **58**, 1982.
2 H.-L. Cheng and K.-F. Lin, *J. Polym. Res.*, 1999, **6**, 123; H.-L. Cheng and K.-F. Lin, *Synth. Met.*, 2001, **122**, 387; H.-L. Cheng and K.-F. Lin, *J. Mater. Chem.*, 2002, **12**, 2270; C.-C. Chiu, K.-F. Lin and H.-L. Chou, *J. Polym. Sci., Part A: Polym. Chem.*, 2003, **41**, 2180; Y.-L. Fan and K.-F. Lin, *J. Polym. Sci., Part A: Polym. Chem.*, 2005, **43**, 2520; H.-L. Chou, K.-F. Lin, Y.-L. Fan and D.-C. Wang, *J. Polym. Sci., Part B: Polym. Phys.*, 2005, **23**, 1705.
3 A. F. M. Kilbinger and W. J. Feast, *J. Mater. Chem.*, 2000, **10**, 1777.
4 A. P. H. J. Schenning, A. F. M. Kilbinger, F. Biscarini, M. Cavallini, H. J. Cooper, P. J. Derrick, W. J. Feast, R. Lazzaroni, Ph. Leclere, L. A. McDonell, E. W. Meijer and S. C. J. Meskers, *J. Am. Chem. Soc.*, 2002, **124**, 1269.
5 O. Henze, D. Parker and W. J. Feast, *J. Mater. Chem.*, 2003, **13**, 1269.
6 A. Gesquière, P. Jonkheijm, A. P. H. J. Schenning, E. Mena Osteritz, P. Bäuerle, S. De Feyterc, F. C. De Schryver and E. W. Meijer, *J. Mater. Chem.*, 2003, **13**, 2164.
7 F. S. Precup-Blaga, A. P. H. J. Schenning and E. W. Meijer, *Macromolecules*, 2003, **36**, 565.
8 Ph. Leclere, M. Surin, P. Jonkheijm, O. Henze, A. P. H. J. Schenning, F. Biscarini, A. C. Grimsdale, W. J. Feast, E. W. Meijer, K. Mullen, J. L. Bredas and R. Lazzaroni, *Eur. Polym. J.*, 2004, **40**, 885.
9 D. G. Bucknull and H. L. Anderson, *Science*, 2003, **302**, 1904.
10 S. Förster and M. Antonietti, *Adv. Mater.*, 1998, **10**, 195.
11 S. Peleshanko, J. Jeong, R. Gunawidjaja and V. V. Tsukruk, *Macromolecules*, 2004, **37**, 6511.
12 Y. Y. Huang, H. L. Chen and T. Hashimoto, *Macromolecules*, 2003, **36**, 764.
13 P. Busch, D. Posselt, D. M. Smilgies, B. Rheinla1nder, F. Kremer and C. M. Papadakis, *Macromolecules*, 2003, **36**, 8717.
14 M. M. Alam, Y. Zhu and S. A. Jenekhe, *Langmuir*, 2003, **19**, 8625.
15 G. Kickelbick, J. Bauer, N. Hüsing, M. Andersson and A. Palmqvist, *Langmuir*, 2003, **19**, 3198.
16 B. W. Messmore, J. F. Hulvat, E. D. Sone and S. I. Stupp, *J. Am. Chem. Soc.*, 2004, **126**, 14452.
17 A. K. Brannan and F. S. Bates, *Macromolecules*, 2004, **37**, 8816.
18 R. B. Prince, J. G. Saven, P. G. Wolynes and J. S. Moore, *J. Am. Chem. Soc.*, 1999, **121**, 3114.
19 M. P. Nieh, S. K. Kumar, R. H. Fernando, R. H. Colby and J. Katsaras, *Langmuir*, 2004, **20**, 9061.
20 M. S. Gin, T. Yokozawa, R. B. Prince and J. S. Moore, *J. Am. Chem.Soc.*, 1999, **121**, 2643.
21 L. Brunsveld, H. Zhang, M. Glasbeek, J. A. J. M. Vekemans and E. W. Meijer, *J. Am. Chem. Soc*, 2000, **122**, 6175.
22 L. Gehringer, C. Bourgogne, D. Guillon and B. Donnio, *J. Am. Chem.Soc.*, 2004, **126**, 3856.
23 B. K. Cho, A. Jain, S. M. Gruner and U. Wiesner, *Science*, 2004, **305**, 1598.
24 C. Koulic and R. Jérôme, *Macromolecules*, 2004, **37**, 888.
25 G. Wang, X. Tong and Y. Zhao, *Macromolecules*, 2004, **37**, 8911.
26 S. Zheng, C. Tao, Q. He, H. Zhu and J. Li, *Chem. Mater.*, 2004, **16**, 3677.
27 M. Lackinger, S. Griessl, T. Markert, F. Jamitzky and W. M. Heckl, *J. Phys. Chem. B*, 2004, **108**, 13652.
28 S. Park, J. H. Lim, S. W. Chung and C. A. Mirkin, *Science*, 2004, **303**, 348.
29 M. Lee, S. J. Lee and L. H. Jiang, *J. Am. Chem. Soc.*, 2004, **126**, 12724.
30 M. Kuang, H. Duan, J. Wang and M. Jiang, *J. Phys. Chem. B.*, 2004, **108**, 16023.
31 M. Lee, C. J. Jang and J. H. Ryu, *J. Am. Chem. Soc.*, 2004, **126**, 8082.
32 D. Yan, Y. Zhou and J. Hou, *Science*, 2004, **303**, 65.
33 H. R. Allcock, E. S. Powell and Y. Chang, *Macromolecules*, 2004, **37**, 7163.
34 F. Jiilicher, U. Seifert and R. Lipowsky, *J. Phys. II*, 1993, **3**, 1681.
35 D. J. Pochan, Z. Chen, H. Cui, K. Hales, K. Qi and K. L. Wooley, *Science*, 2004, **306**, 94.
36 J. F. Hulvat, M. Sofos, K. Tajima and S. I. Stupp, *J. Am. Chem. Soc.*, 2005, **127**, 366.
37 J. S. Beck, J. C. Vartuli, W. J. Roth, M. E. Leonowicz, C. T. Kresge, K. D. Schmitt, C. T.-W. Chu, D. H. Olson, E. W. Sheppard, S. B. McCullen, J. B. Higgins and J. L. Schlenker, *J. Am. Chem. Soc.*, 1992, **114**, 10834.
38 M. Grätzel, *Nature*, 2001, **414**, 338.
39 Q. L. Fan, S. Lu, Y. H. Lai, X. Y. Hou and W. Huang, *Macromolecules*, 2003, **36**, 6976.
40 A. Drury, S. Maier, M. Rüther and W. J. Blau, *J. Mater. Chem.*, 2003, **13**, 485.
41 M. R. Pinto, B. Hu, F. E. Karasz and L. Akcelrud, *Polymer*, 2000, **41**, 8095.
42 K.-F. Lin and W.-Y. Shu, *Polymer*, 1994, **16**, 3535.

